iScience

CellPress
OPEN ACCESS

Article

Semen promotes oocyte development in *Sebastes schlegelii* elucidating ovarian development dynamics in live-bearing fish

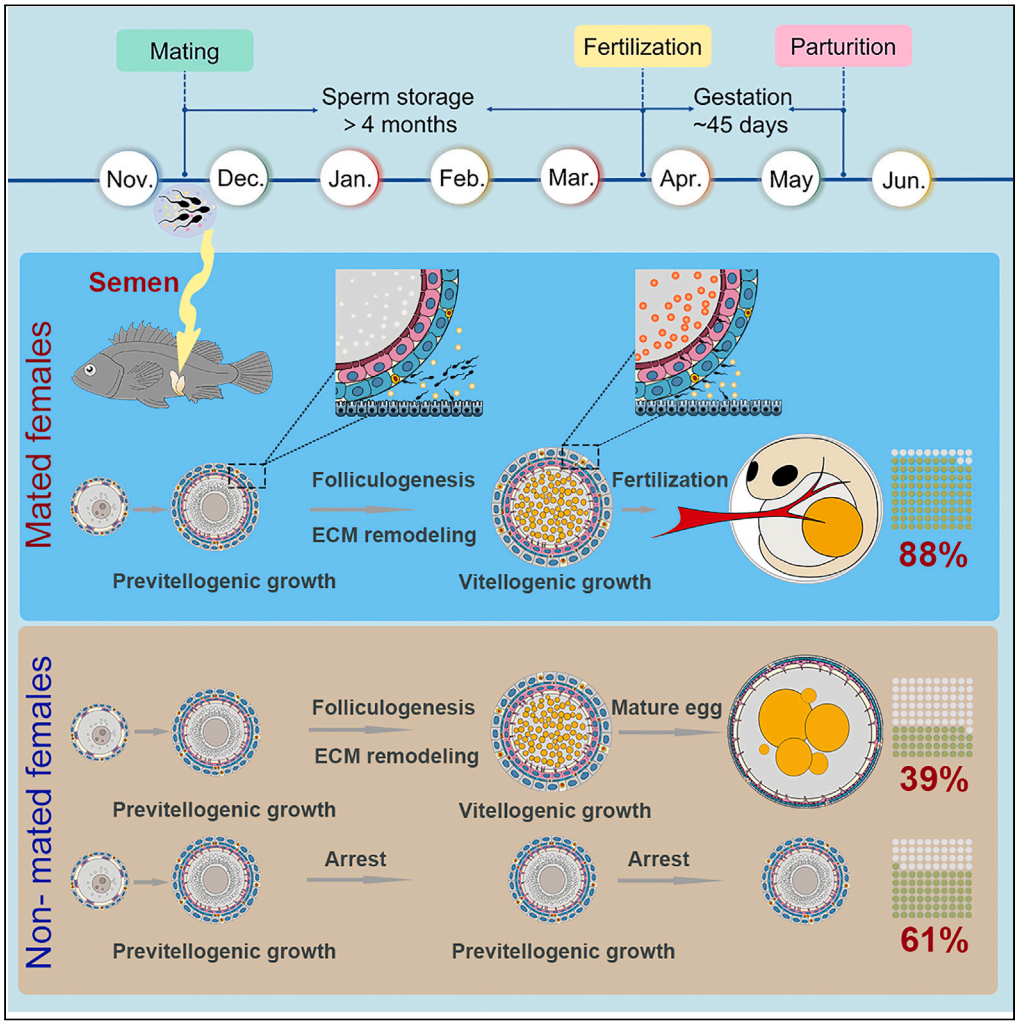

Fengyan Zhang, Weihao Song, Ruiyan Yang, ..., Jie Qi, Quanqi Zhang, Yan He

yanhe@ouc.edu.cn

Highlights

Semen promotes oocyte development in a viviparous teleost, *Sebastes schlegelii*

Semen influences female follicular cell remodeling

Semen induces brain feedback, stimulating oocyte maturation

Zhang et al., iScience *27*, 109193
March 15, 2024
https://doi.org/10.1016/j.isci.2024.109193

iScience

CellPress
OPEN ACCESS

Article

Semen promotes oocyte development in *Sebastes schlegelii* elucidating ovarian development dynamics in live-bearing fish

Fengyan Zhang,[1] Weihao Song,[1] Ruiyan Yang,[1] Chaofan Jin,[1] Yuheng Xie,[1] Yiyang Shen,[1] Xiangyu Gao,[1] Hao Sun,[1] Tianci Nie,[1] Xinlu Yue,[2] Zongcheng Song,[2] Jie Qi,[1] Quanqi Zhang,[1,2] and Yan He[1,3,*]

SUMMARY

In some vertebrates and invertebrates, semen release factors affecting female physiology and behavior. Here, we report that semen delivered to females is potentially beneficial for promoting oocyte development in a viviparous teleost, *Sebastes schlegelii*. 88% of mated ovaries develop normally and give birth to larval fish, whereas 61% of non-mated ovaries are arrested in the previtellogenic stage. Semen's significant role ($p < 0.0001$) in promoting oocyte development may involve remodeling follicular cells and regulating the expression of the extracellular matrix, which facilitates cell communication. Furthermore, the ovarian response to semen may influence the brain, affecting hormone release, follicular cell development and steroid production, and crucial for oocyte growth. This mechanism, which could potentially delay maternal investment in offspring until male genetic input occurs to avoid energy wastage, has not been previously described in teleosts. These findings enhance our understanding of ovarian development in viviparous fish, with broader implications for reproductive biology.

INTRODUCTION

Species that fertilize externally typically produce mature gametes of both sexes synchronously, with sperm chemotaxis to eggs ensuring fertilization.[1,2] In contrast, animals with internal fertilization benefit from the female's ability to store sperm, enabling fertilization even when gamete maturation is asynchronous.[3] Post-mating, semen and ovarian communication at the cellular and molecular levels are key components for successful reproduction. In several insect species, semen has been proven to be necessary for inducing ovulation[4–6] or advancing the development of immature oocytes.[7,8] In two sessile marine invertebrates, sperm stimulates oocyte vitellogenesis and maturation.[9] Similarly, in mammals such as camels and alpacas, the existence of β nerve growth factor (β-NGF) in semen elicits an ovulatory response in females.[10,11]

In teleosts, about 500 out of 30,000 species are viviparous,[12] utilizing a variety of strategies to store sperm in the ovaries.[12,13] The black rockfish, *Sebastes schlegelii*, an important commercial fishery, which belongs to the *Sebastes* genus in the Sebastidae family, inhabits the coasts of Japan, South Korea, and China.[14] It is a viviparous teleost with asynchronous gonadal development between two sexes and long-term sperm storage.[15] Spermatogenesis begins in June, and mature sperm are produced in November.[15] Mating usually occurs in November and December, when the ovaries develop at the previtellogenic stage. After mating, mature sperm enter the ovarian cavity and are stored for at least four months.[12] Oocytes undergo vitellogenic and maturation stages from December to the following March, and eventually produce mature eggs ready for fertilization in the following March-April. After fertilization, the embryos develop in the follicular placenta and are dependent on both yolk and maternal nutrition.[16] The ovaries give birth to larval fish and subsequently regress in the following May. During the reproductive seasons of *S. schlegelii*, we previously found that the ovaries of the non-mated females exhibited arrested development and failed to mature. A previous study also observed that the abnormal spawning of female *S. schlegelii* occurs in the absence of copulation during the mating season.[17] Whether semen could promote oocyte development in viviparous teleost fish, *S. schlegelii*, to our knowledge, is undescribed.

In this study, we demonstrated the role of semen in promoting oocyte development in *S. schlegelii*. By integrating our observations of morphology and molecular data, we proposed a hypothetical model to explain the effects of semen on oocyte development in *S. schlegelii*. Our findings contribute to a better understanding of the mechanisms underlying ovarian development in viviparous fish.

[1]MOE Key Laboratory of Marine Genetics and Breeding, College of Marine Life Sciences/Sanya Oceanographic Institution, Ocean University of China, Qingdao 266000/Sanya 572000, Shandong/Hainan, China
[2]Weihai Shenghang Ocean Science and Technology Co., Ltd, Weihai, Shandong 264200, China
[3]Lead contact
*Correspondence: yanhe@ouc.edu.cn
https://doi.org/10.1016/j.isci.2024.109193

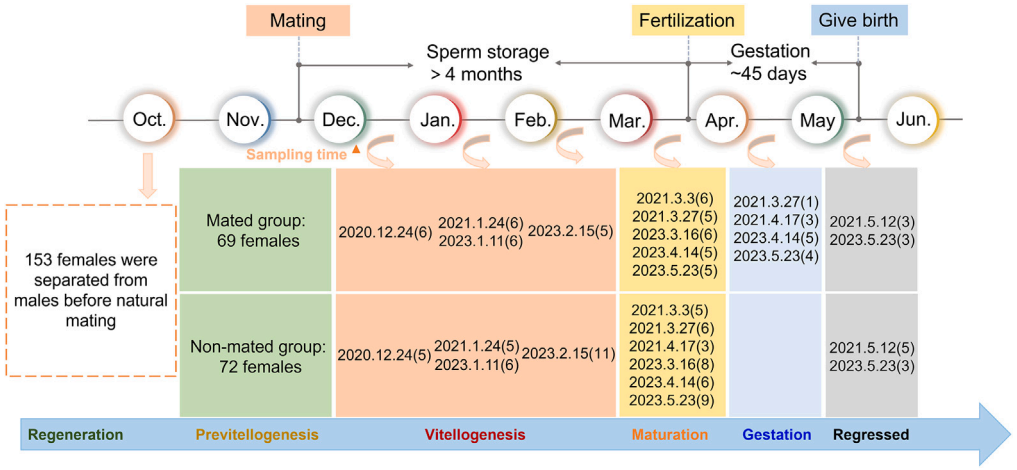

Figure 1. The experimental design involved the artificial insemination of *S. schlegelii*

The numbers in parentheses represent the sampling size of females at different developmental stages of each group. Previtellogenic stage states samples collected on 2020.11.28 and 2022.11.24; Vitellogenic stage demonstrates samples collected on 2020.12.24, 2021.1.24, 2023.1.11 and 2023.2.15; Maturation stage represents samples collected on 2021.3.3, 2021.3.27, 2021.4.17, 2023.3.16, 2023.4.14 and 2023.5.23; Gestation stage displays samples collected on 2021.3.27, 2021.4.17, 2023.4.14 and 2023.5.23, and all are embryos; Regressed stage shows samples collected on 2021.5.12 and 2023.5.23.

RESULTS

Morphological differences of ovaries in the mated and non-mated groups of *S. schlegelii*

The experimental design for the artificial insemination of *S. schlegelii* is shown in Figure 1. The degree of ovarian development was significantly different between the mated and non-mated groups at the same developmental stages through a visual comparison of ovarian appearance (Figure 2A). In the mated group, ovaries could reach the weight of 31.81 ± 22.56 and 59.40 ± 12.51 g at the pre-fertilization (collected on 2021.3.3 and 2023.3.16) stage and the weight of 135.53 ± 47.27 and 136.76 ± 37.68 g at the gestation (collected on 2021.4.17 and 2023.4.14) stage. Only eight mated ovaries were smaller, slender, and arrested developed whereas the remaining 61 mated ovaries were big and normally developed at the same development stage (Figures 2C; Table S1). To be noted, in the non-mated group, at any stage, approximately 61% of the ovaries (44/72) remained comparable in weight to the pre-mated ovaries, and the ovarian maturation index was around 0.01, representing arrested development. Furthermore, the other 28 ovaries in the non-mated group had similar weights to the normally developed mated ovaries at the same development stage and were also capable of producing mature eggs at the maturation (2023.4.14, 2023.5.23) stage (Figures 2C, Table S1, and Figure S3). The GSI also showed significantly differences between normally developed mated ovaries and arrested developed non-mated ovaries at the same developmental stages, whereas the GSI of the mated and non-mated groups with normally developed ovaries had no differences (Figure S1). Furthermore, the chi-square test of semen (mated and non-mated groups) confirmed that the role of semen in promoting oocyte development was significant (Figure 2C).

Furthermore, we conducted a comprehensive investigation into sperm storage in both the mated and non-mated groups, regardless of normal or arrested development. We found sperm to be present in all the normally developed mated ovaries whereas no sperm was found in the non-mated ovaries regardless of normal or arrested development. Moreover, we were unable to detect the presence of sperm in the ovaries with arrested development in the mated group. The sperm storage information was listed in Table S1. At the pre-fertilization stage, the sperm were stored in the epithelial cells which were proliferating and located in the outer layer of follicular cells[13] (Figure S2). Moreover, the normally developed non-mated ovaries could develop into vitellogenic and maturation stage, which had similar histological dynamics to the mated group with normally development ovaries (Figure S3). Nevertheless, significant histological differences were observed between normally developed mated ovaries and arrested developed non-mated ovaries at the same developmental stages (Figure 2B). The staging standard of ovaries and oocytes was based on previous studies conducted in *S. schlegelii*.[15,18] In the pre-mated group, most ovaries were at the previtellogenic stage, characterized by an increased number of oil droplets. The oocytes developed from the primary growth (PG) phase to the early secondary growth (SGe) phase, surrounded by follicular cell layers that increased from one to two layers (Figure 2a). At the post-mating and pre-fertilization stages, almost all of the mated ovaries developed into vitellogenic and maturation stages. The Oocytes were at the late secondary growth (SGl) phase and full secondary growth (SGf) phase, still enveloped by two-layered follicular cells, and showed the accumulation and maturation of yolk granules (Figure 2b–f). However, at the same developmental stages, most of the non-mated ovaries retained in previtellogenic stage with not fully developed follicular cell layers (Figure 2b′–f′). At the post-fertilization and post-gestation stages, almost all of the mated ovaries gave birth to larval fish and subsequently regressed (Figure 2g–i). In contrast, most of the non-mated ovaries stayed arrested status (Figure 2g′–i′). The regressed ovaries in the mated group at the post-gestation stage displayed abundant blood vessels and residual oocytes at the PG phase, while the oocytes in the non-mated ovaries showed follicular atresia, with autophagic vacuoles gradually formed and became numerous in the follicular cells and the oocytes were phagocytized and removed[19] (Figure 2i, i′).

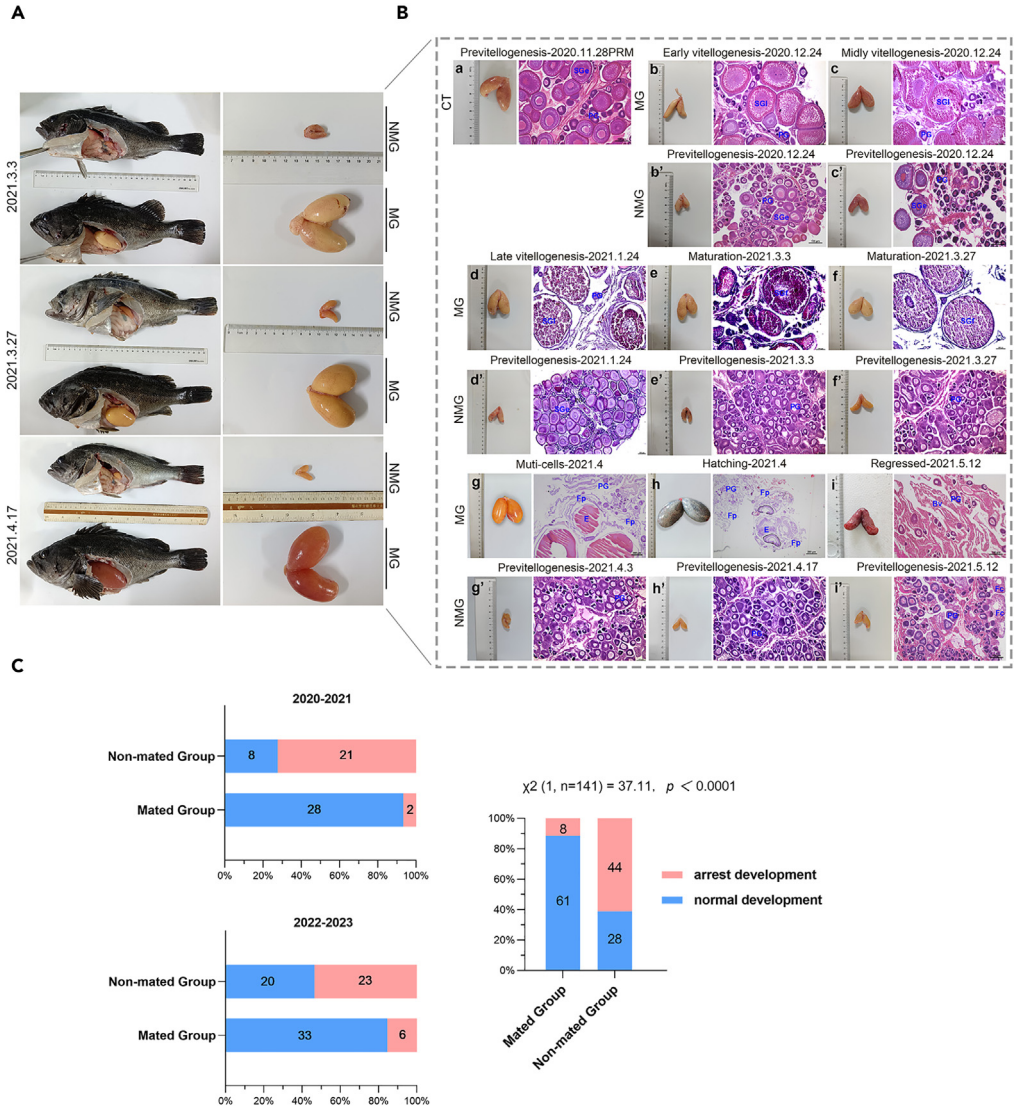

Figure 2. Morphological statistics and hematoxylin-eosin staining were performed on ovaries at different developmental stages in the three groups (CT, MG, NMG) of *S. schlegelii*

Significant promotion of oocyte development through semen stimulation was analyzed in two replicates of artificial insemination experiment.

(A) A visual comparison of fish body and ovarian appearance was made between the normally developed mated and arrested developed non-mated ovaries at the pre-fertilization (2021.3.3, 2021.3.27) and post-fertilization (2021.4.17) stages.

(B) The groups are categorized as follows: CT, the pre-mated group or control group (a); MG, the mated group with normally developed ovaries (b, c, d, e, f, g, h, i); NMG, the non-mated group with arrested developed ovaries (b′, c′, d′, e′, f′, g′, h′, i′). PG, oocyte at the primary growth phase; SGe, oocyte at the early secondary growth phase; SGl, oocyte at the late secondary growth phase; SGf, oocyte at the full secondary growth phase; Bv, blood vessel; Fp, follicular placenta; E, embryo; Fc, follicular cells with autophagic vacuoles. Scale bars are shown in the pictures.

(C) The statistical analysis was performed on the normally developed and arrested developed ovaries in the mated and non-mated groups, including two replicates of artificial insemination experiment in 2020 and 2022. Chi-square test of semen (mated and non-mated groups) was conducted.

Through morphological analysis and histological observations, we revealed that almost all of the mated ovaries matured normally and gave birth to larval fish whereas 61% of the ovaries in the non-mated group exhibited arrested development and were retained in the pre-vitellogenic stage in *S. schlegelii*.

Ultrastructural analysis of ovaries in the mated and non-mated groups of *S. schlegelii*

Comparative analysis of ovarian ultrastructure was investigated by TEM between normally developed mated ovaries and arrested developed non-mated ovaries of *S. schlegelii* at the vitellogenic and maturation stages (Figure 3). The surface of oocytes from the normally developed

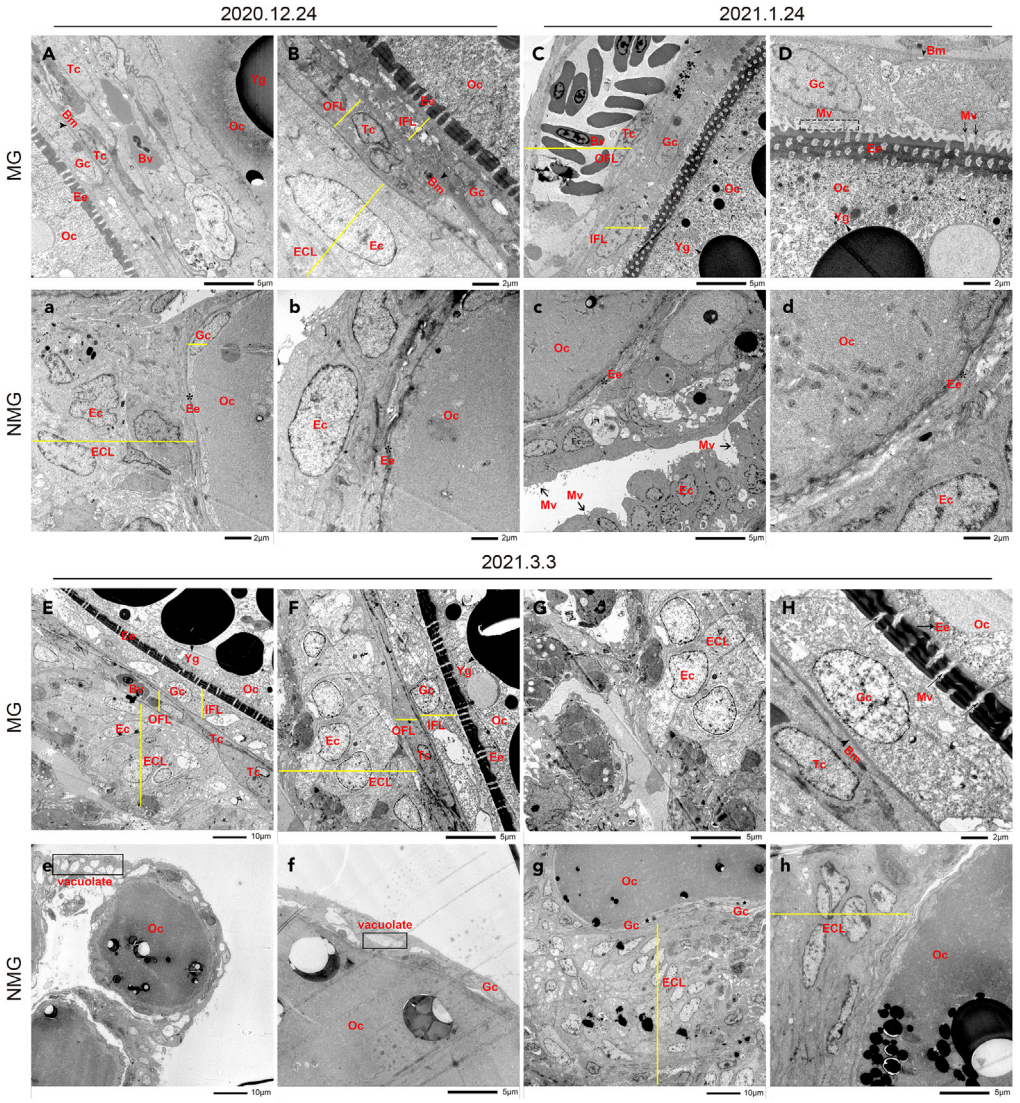

Figure 3. Ultrastructural analysis using TEM in the normally developed mated and arrested developed non-mated ovaries of *S. schlegelii* at different developmental stages

MG, the mated group (A–H); NMG, the non-mated group (a–h). 2020.12.24 and 2021.1.24 represent the vitellogenic stage while 2021.3.3 states the maturation stage. Oc, oocyte; Yg, york granule; Gc, granulosa cell; Tc, theca cell; Bm, basement membrane; Ee, egg envelope; Ec, epithelial cell; IFL, inner follicular layer; OFL, outer follicular layer; ECL, epithelial cell layer; Mv, microvilli; Bv, blood vessel; vacuolate. Scale bars are shown in the pictures.

mated ovaries consisted of three layers from the inside to the outside: granulosa cells, theca cells, and epithelial cells (Figures 3B, 3C, 3E, and 3F). The granulosa cells surrounding a basement membrane together with the theca cells which were vascularized comprised of the follicular cells (Figures 3A–3D). However, the oocytes from the arrested developed non-mated ovaries were surrounded by two layers, an inner follicular cell layer and an outer epithelial cell layer. The follicular cells exhibited incomplete development, with only one cell layer or even missing (Figures 3a, 3g, and 3h). The egg envelope in the normally developed mated ovaries appeared significantly thicker, with numerous small holes penetrated by microvilli present on the egg envelope and the granulosa cells (Figures 3D and 3H). In contrast, the egg envelope in the normally developed non-mated ovaries was underdeveloped, appearing extremely thin or even invisible (Figures 3b–3d). Moreover, in the mated group with normally developed ovaries, as the ovaries developed, the epithelial cells gradually proliferated and thickened, primarily adopting a columnar shape, while the granulosa cells became rounder and larger, and the theca cells were compressed and narrowed (Figures 3E–3G). In the non-mated group with arrested developed ovaries, vacuolate follicular cells were observed on the oocyte surface, and the epithelial cells exhibited excessive proliferation and occupied the majority of ovarian cells (Figures 3e–3g). Additionally, the ovarian follicular apoptosis in *S. schlegelii* was analyzed by TUNEL assay, comparing normally developed mated ovaries and arrested developed non-mated ovaries at different developmental stages (Figure S4). Out of 23 arrested developed non-mated ovaries examined, follicular apoptosis was found in only

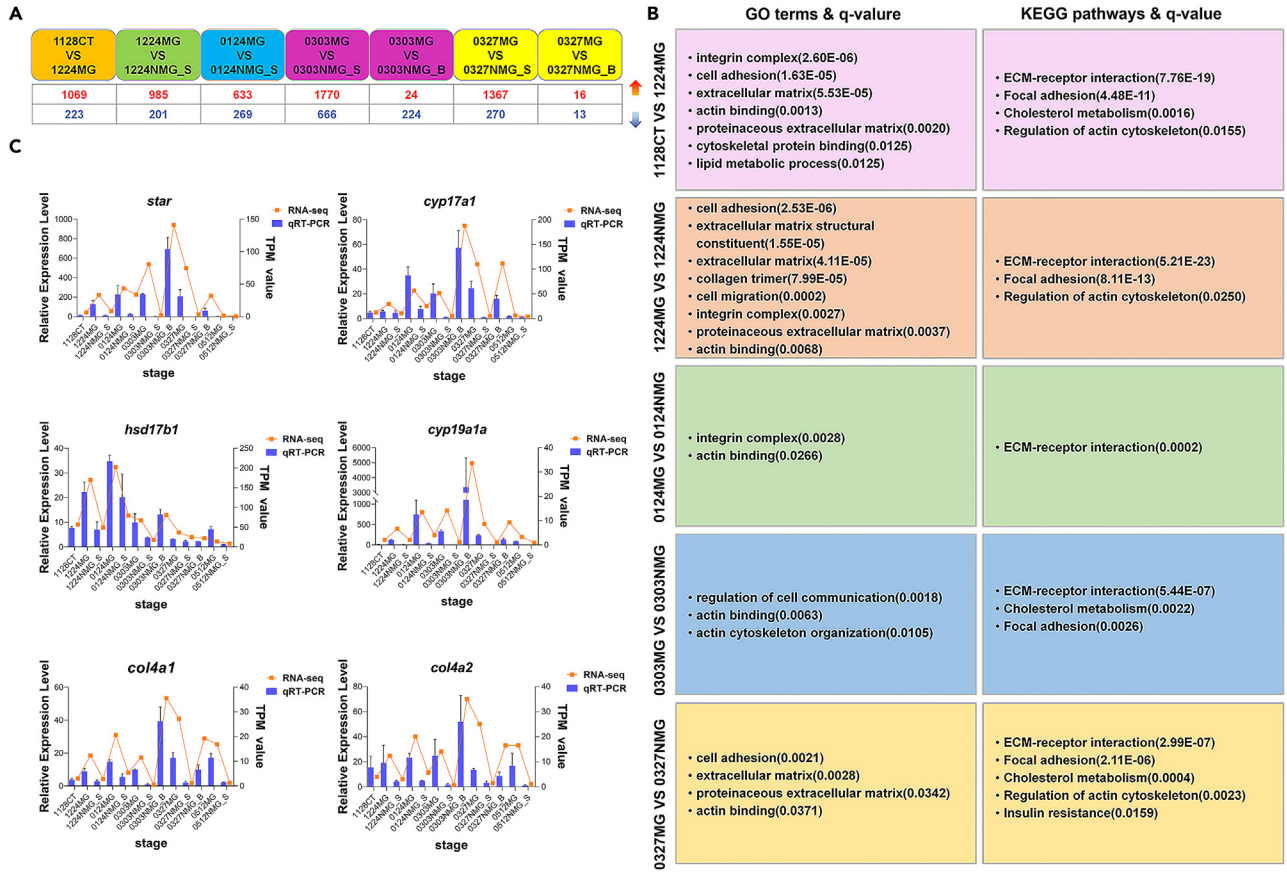

Figure 4. Identification of differentially expressed genes (DEGs) between the mated and non-mated ovaries of *S. schlegelii* at different developmental stages

(A) Up-regulation (red) and down-regulation (blue) of DEGs in the ovaries of the three groups (CT, MG and NMG) at different developmental stages.

(B) Selected enriched GO terms and KEGG pathways of top 30 in 1128CT VS 1224MG, 1224MG VS 1224NMG, 0124MG VS 0124NMG, 0303MG VS 0303NMG and 0327MG VS 0327NMG, the figures in parentheses represent q-value. All mated ovaries are normally developed and all non-mated ovaries are arrested development in here.

(C) The expression patterns of selected DEGs in the ovaries of the three groups (CT, MG and NMG) revealed by qRT-PCR and RNA-seq. Data are mean ± SD. The folded diagram shows the gene expression pattern based on TPM value, the bar chart shows the gene expression pattern relative to *rpl17*. CT, the pre-mated group or control group; MG, the mated group with normally developed ovaries; NMG_S, the non-mated group with arrested developed ovaries; NMG_B, the non-mated group with normally developed ovaries. The numeral prefix of each group indicates the sampling time.

one non-mated individual. This finding further confirmed that in the majority of the arrested ovaries, the follicular structure was poorly developed, rather than undergoing degradation due to the absence of semen.

Using TEM and TUNEL assay, we observed that the follicular cells, including both granulosa and theca cells, could normally develop in the normally developed mated ovaries. However, in the arrested developed non-mated ovaries, the follicular cells were poorly developed.

Different gene expression profiles of ovaries in the mated and non-mated groups of *S. schlegelii*

In this study, forty-five libraries were successfully constructed and sequenced. The gene differential expression analysis was performed on the ovaries of the three groups (CT, MG, NMG) at different developmental stages in *S. schlegelii* (Figure 4A). For the normally developed mated ovaries and arrested developed non-mated ovaries, at the vitellogenic (2020.12.24, 2021.1.24) and maturation (2021.3.3, 2021.3.27) stages, 985, 633, 1770, and 1367 DEGs were down-regulated in the non-mated group, respectively. Nevertheless, only 248 and 29 DEGs were respectively found at the maturation (2021.3.3, 2021.3.27) stage between normally developed ovaries in both mated and non-mated groups. To confirm these differences were due to individual variations, clustering analysis of gene expression profiles was also performed between the mated and non-mated ovaries of *S. schlegelii* at the maturation stage (2021.3.3 and 2021.3.27) (Figure S5). Principal component analysis (PCA) and hierarchical clustering showed that the ovaries were classified into two clusters, normally developed ovaries and arrested developed ovaries. The normally developed mated ovaries clustered together with normally developed ovaries of the non-mated group, while the arrested developed ovaries of the non-mated group formed a separate cluster.

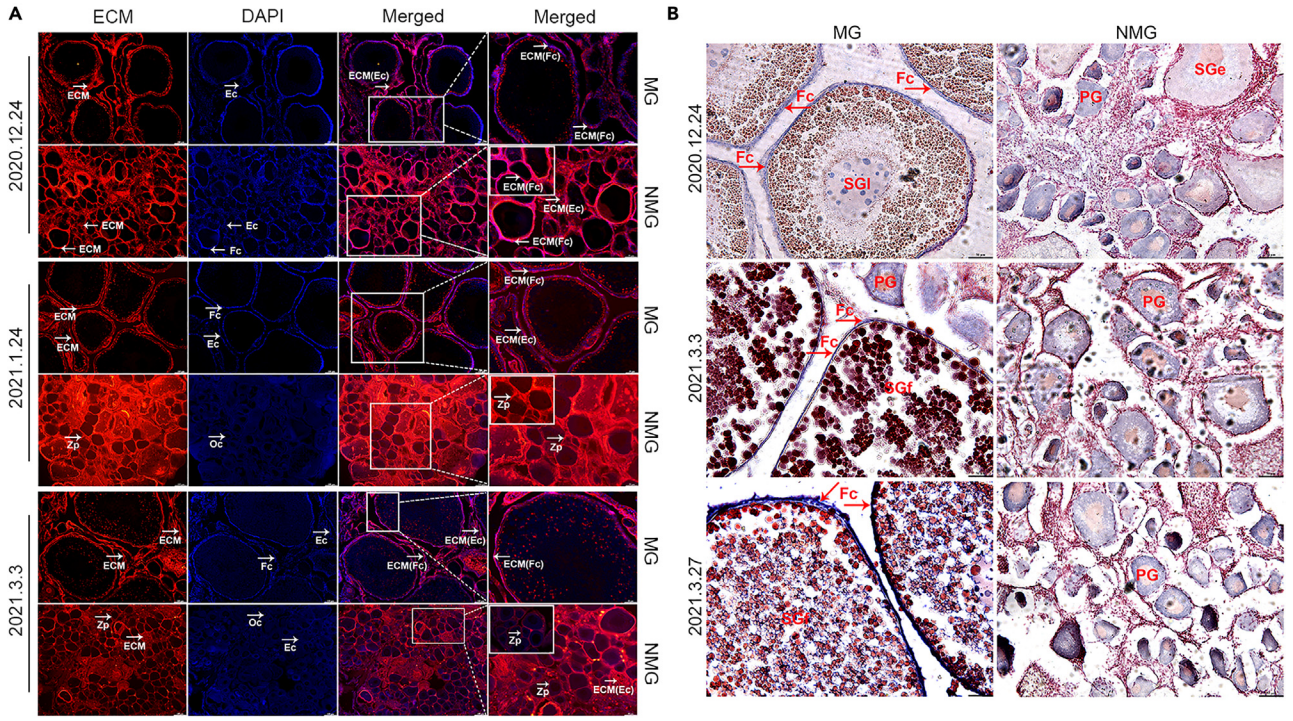

Figure 5. ECM distribution in the ovaries

ECM distribution revealed by wheat germ agglutinin (WGA) staining (A) and *in situ* hybridization (ISH) of *col4a1* (B) in the normally developed mated and arrested developed non-mated ovaries of *S. schlegelii* at different developmental stages.

ISH is performed with DIG-labeled *col4a1* anti-sense probes as positive signals or sense probes as negative controls. The positive signals are showed as blue and the negative controls show no positive signals in Figure S8. MG, the mated group; NMG, the non-mated group. Oc, oocyte; ECM, extracellular matrix; Ec, epithelial cell; Zp, zona pellucida; Fc, follicular cell; PG, oocyte at the primary growth phase; SGl, oocyte at the late secondary growth phase; SGf, oocyte at the full secondary growth phase. Numbers represent the sampling time. Scale bar = 100 μm, 50 μm, 20 μm. Magnified views in the white boxes.

To further investigate the function of these DEGs, gene ontology (GO) and kyoto encyclopedia of genes and genomes (KEGG) enrichment analyses of DEGs were performed (Figure 4B). Significantly enriched GO terms for molecular functions included cytoskeletal protein binding, actin binding and extracellular matrix structural constituent. Significantly enriched GO term for biological processes encompassed cell adhesion, cell migration, actin cytoskeleton organization, and regulation of cell communication. Moreover, significantly enriched GO term for cellular components included extracellular matrix, proteinaceous extracellular matrix, integrin complex, and collagen trimer. Besides, the KEGG pathway enrichment analysis revealed significant enrichment in pathways such as focal adhesion, regulation of actin cytoskeleton, ECM-receptor interaction, cholesterol metabolism and insulin resistance. To validate the expression levels of the screened DEGs, qRT-PCR were utilized to confirm their expression patterns. Six DEGs, including *star*, *hsd17b1*, *cyp17a1*, *cyp19a1a*, *col4a1*, and *col4a2* were selected for validation. The results demonstrated consistent expression patterns between the RNA-seq and qRT-PCR data (Figure 4C).

ECM distribution in the ovaries examined by wheat germ agglutinin staining and *in situ* hybridization in the mated and non-mated groups of *S. schlegelii*

"ECM-receptor interaction" was significantly enriched of DEGs, hence the detailed distribution of the extracellular matrix (ECM) of *S. schlegelii* between normally developed mated ovaries and arrested developed non-mated ovaries at different developmental stages were examined through wheat germ agglutinin (WGA) staining (Figures 5A and S6). WGA, a group of isolectins, selectively binds to N-acetyl-D-glucosamine and N-acetylneuraminic acid (sialic acid) residue. Fluorescently labeled WGA staining is widely used for detecting, visualizing, and quantifying fibrotic or connective tissue in animals.[20–22] In this study, the fluorescent WGA probe was utilized for the first time to display the distribution of the ECM in fish ovaries. The results showed abundant WGA-positive signals between the follicular cells on the oocyte surface at the PG, SGe, SGl, and SGf phases, as well as between the surrounding somatic cells, such as epithelial cells in the normally developed mated ovaries (Figure 5A and S6). DAPI staining demonstrated that the follicular cell layers were normally developed in the normally developed mated ovaries, with one layer of follicular cells at the PG stage and two layers of follicular cells at the SGe, SGl, and SGf phases (Figures 5A and S6). Nevertheless, in the arrested developed non-mated ovaries, the ECM between the follicular cells was absent, and the surface of the oocyte lacked follicular cells at the PG or SGe phase. Notably, WGA-positive signals were also pronounced between the surrounding somatic cells, such as epithelial cells, in the arrested developed non-mated ovaries (Figures 5A and S6). Furthermore, the distribution of type IV collagen of *S. schlegelii* between normally

developed mated ovaries and arrested developed non-mated ovaries at different developmental stages was examined through ISH of *col4a1* (Figure 5B). The results revealed significant *col4a1* expression in the follicular cells of the normally developed mated ovaries, whereas it was only expressed in the cytoplasm of oocytes at the PG and SGe phases in the arrested developed non-mated ovaries.

In summary, the ECM was abundant between the follicular cells and the surrounding somatic cells, such as epithelial cells, in the normally developed mated ovaries. Similarly, the ECM was abundant between the surrounding somatic cells in the arrested developed non-mated ovaries, but the ECM between the follicular cells was largely absent.

Expression of sex steroid hormone-related genes in the ovaries of mated and non-mated groups of *S. schlegelii*

"Cholesterol metabolism" was significantly enriched of DEGs. Therefore, key genes involved in cholesterol metabolism, such as *star*, *cyp17a1*, *hsd17b1*, and *cyp19a1a*, were investigated at different developmental stages in the CT, MG with normally developed ovaries and NMG with arrested developed ovaries of *S. schlegelii* (Figures 6 and S7). These genes showed significantly different expression patterns between normally developed mated ovaries and arrested developed non-mated ovaries at the corresponding developmental stages. In the pre-mated group, during the previtellogenic stage, *star* and *cyp17a1* were expressed in the cytoplasm of oocytes at the PG and SGe phases (Figures S7A and S7B). The expression level of *hsd17b1* was relatively low in the cytoplasm of oocytes at the PG phase, but it showed a significantly increase in the granulosa cells at the SGe phase (Figure S7D). *cyp19a1a* showed high expression level in the cytoplasm of oocytes at the PG and SGe phases, and lower expression levels in the follicular cells at the SGe phase and surrounding somatic cells, such as epithelial cells (Figure S7C). In the normally developed mated ovaries, during the vitellogenic and maturation stages of the ovaries, *star* and *cyp19a1a* were predominantly expressed in the granulosa cells, as well as theca cells at the SGI and SGf phases. Signals of *Star* and *cyp19a1a* were also detected in somatic cells, such as epithelial cells (Figures 6A and 6D). *cyp17a1* was highly expressed in both the granulosa and theca cells, with the increasing expression level as the ovary developed (Figure 6B). *hsd17b1* exhibited specific high expression in the granulosa cells (Figure 6C). Notably, all these genes were expressed in the cytoplasm of PG oocytes at the vitellogenic, maturation and regressed stages. However, in the arrested developed non-mated ovaries, the ovaries retained in the previtellogenic stage. *star*, *cyp17a1*, *hsd17b1* and *cyp19a1a* were not expressed in the follicular cells because of the missing of follicular cell layers (Figures 6A–6D). Signals of *Star* and *cyp19a1a* were mainly observed in the cytoplasm of oocytes at the PG and SGe phases. *cyp19a1a* also showed weak expression in the somatic cells, such as epithelial cells. *Cyp17a1* and *hsd17b1* were specifically expressed in the cytoplasm of oocytes at the PG stage.

DISCUSSION

Semen could promote oocyte development in *S. schlegelii*

In two replicates of the artificial insemination experiment of *S. schlegelii*, we observed that semen served as a promotive factor, for triggering and sustaining vitellogenesis, and consequently, for ensuring successful reproduction. This result is intriguing and mirrors observations in female red-sided garter snakes (*Thamnophis sirtalis parietalis*), where mating stimuli are known to induce oocyte vitellogenesis.[23,24] However, we encountered arrested ovaries in the mated group and normal developed ovaries in the non-mated group. Notably, sperm was absent in the ovaries with arrested development in the mated group, as well as in all the ovaries of the non-mated group, irrespective of their developmental status. We suspect that the developmental arrest observed in eight individuals from the mated group could be attributed to an unsuccessful artificial semen injection. A previous study indicated a 60% success rate in artificial insemination, potentially impacted by the varying semen quality from different males.[25] To enhance the effectiveness of artificial fertilization in our study, we utilized a mix of semen from multiple males, which reduced the risk associated with compromised semen quality and achieved a success rate of nearly 90%. Although this rate surpasses that of the previous study,[25] certain procedural errors, such as semen leakage post-injection might still occur.

Regarding the normally developed ovaries in the non-mated group, we hold the opinion that many cues stimulate vitellogenesis and promote oocyte development beyond the present of semen. On the one hand, in the non-mated group, we discovered that individuals with normally developed ovaries had significantly ($p < 0.001$) higher weights than those with the arrested development of ovaries. However, this difference was not observed in the mated group. We posit that semen is a promotive factor for oocyte development in the mated group, but some other factors such as a relatively higher weight appears to be a contributor for the initiation of oocyte vitellogenesis in the absence of semen. On the other hand, we observed that the transcriptomes of the normally developed ovaries of the non-mated group were more similar to those of the mated ovaries (with sperm storage). This indicates that if the ovaries can initiate the normal development without the semen trigger, the influence of semen on their transcriptome is minimal, making semen a secondary factor in ovarian development. Factors such as adequate nutrition, endogenous hormonal fluctuations, or even the internal biological clock of the fish could be instrumental in triggering ovarian development.[26–29] This notion is supported by observations in red-sided garter snakes, where environmental cues, physiological conditions, and psychological stressors contribute to ovarian growth beyond mating activities. For example, some non-mated females also become vitellogenic in garter snakes under the harsh environment of northern Canada.[30] In *S. schlegelii*, mating occurs in the cold winter months of November and December, and the ovaries develop at least four months ready for fertilization, which need a huge energy drain.[15,26] At the pre-fertilization stage, the ovarian weight and GSI of females significantly increased, reaching the highest GSI of 0.4. The oocytes were fully developed with the filling of mature yolks, which accumulated a large amount of nutrients and provided a good nutrient environment for fertilization and the development of fertilized eggs. Consequently, early and correct allocation of energy resources is critical, which also assemblies the relationship of survival and gonad development.[31] Arrest of female gonad development after completing vitellogenesis is common in many fish living at high latitudes. This phenomenon depends greatly on both the organisms' sensitivity to environmental stresses and the accuracy of their responses to environmental cues.[31] Based on these observations, we speculate that these females with normally

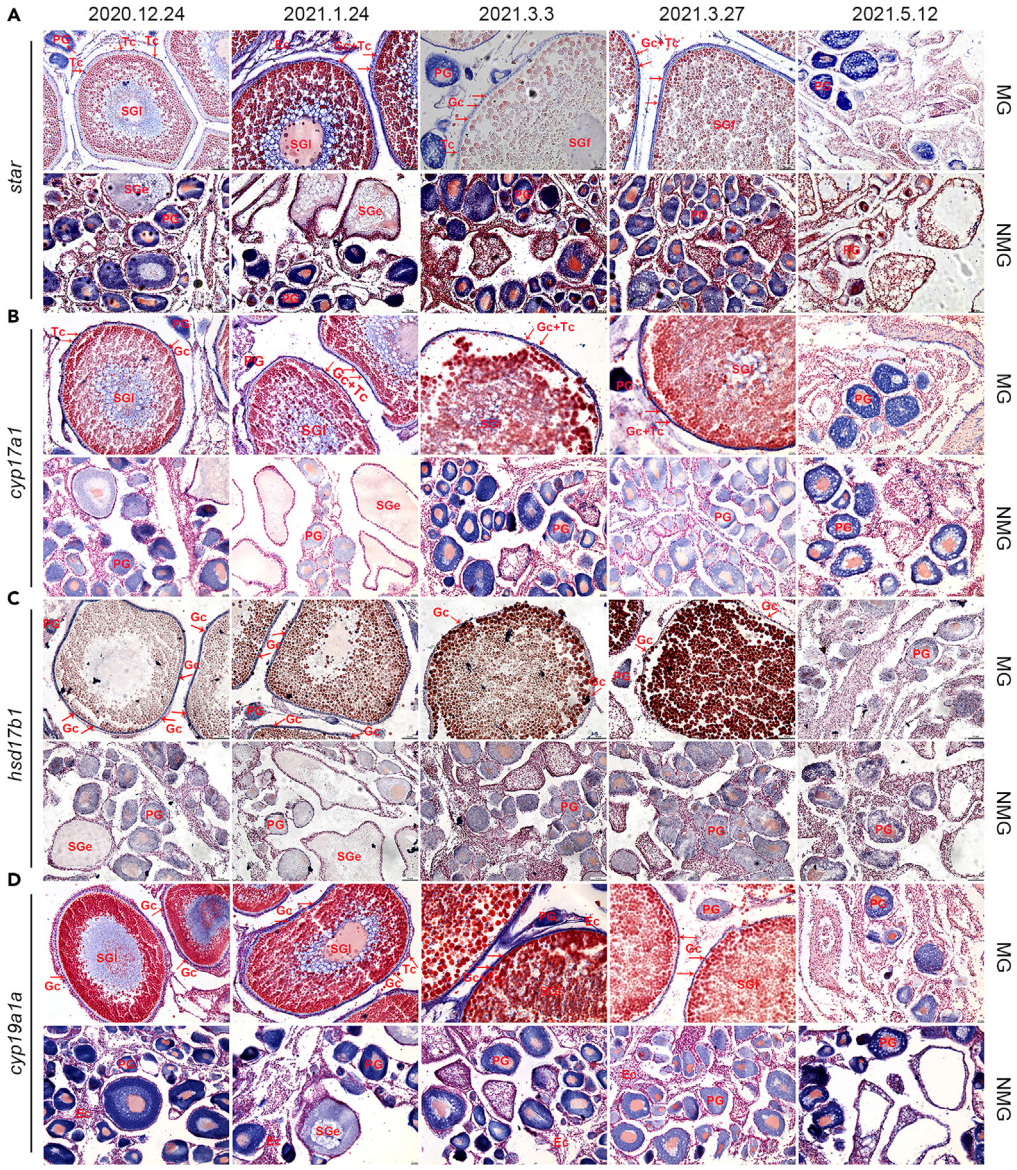

Figure 6. The expression patterns of *star*, *cyp17a1*, *hsd17b1*, and *cyp19a1a* transcripts in the normally developed mated and arrested developed non-mated ovaries of *S. schlegelii* at different developmental stages

In situ hybridization (ISH) are performed with DIG-labeled *star* (A), *cyp17a1* (B), *hsd17b1* (C) and *cyp19a1a* (D) anti-sense probes as positive signals or sense probes as negative controls. The positive signals are showed as blue and the negative controls show no positive signals in Figure S8. MG, the mated group; NMG, the non-mated group. PG, oocyte at the primary growth phase; SGe, oocyte at the early secondary growth phase; SGl, oocyte at the late secondary growth phase; SGf, oocyte at the full secondary growth phase; Gc, granulosa cell; Tc, theca cell; Ec, epithelial cell. Numbers on the top state the sampling time. Scale bars are shown in the pictures.

developed ovaries in the absence of semen have superior energetic states by themselves to support oocyte development, which reflects the evolution to the challenge of the limited environment of these individuals in *S. schlegelii*. Furthermore, genetic predispositions may influence an individual's responsiveness to hormonal cues or environmental conditions, resulting in the capacity for ovarian development. In summary, we believe that the initiation of oocyte development in *S. schlgelii* is influenced by a variety of factors, among which semen plays an important role. The presence of semen offers a potential mechanism whereby the female can ensure the genetic contribution of the male before committing her own resources, thereby optimizing energy expenditure and efficiency in the reproductive process.

Follicular cells play vital roles in regulating oocyte development

Ultrastructural analyses revealed the presence of intact follicular cell layers on the surface of oocytes in the normally developed mated ovaries, whereas the development of follicular cell layers was disrupted in the arrested developed non-mated ovaries. We hypothesize that the

dysplasia of follicular cells is responsible for the arrested development of oocytes in the non-mated ovaries. Through transcriptome data analysis, we identified a critical component, ECM, which probably played a crucial role in the development of ovarian follicular cells. The ECM, consisting of collagens, proteoglycans and glycosaminoglycans, elastins, fibronectins, and laminins, provides essential structural support, regulates tissue development, and maintains organismal homeostasis.[32–34] Numerous studies have confirmed the significant role of ECM in promoting ovarian follicular cells development. For instance, porcine granulosa cells culture on surface coated with type I or IV collagen, fibronectin or laminin, displays promoted attachment ability.[30] Inadequate ECM remodeling results in the loss of follicular structure in murine ovaries.[35] In this study, we observed the expression of type IV collagen in the follicular cells of the normally developed mated ovaries, whereas it was absent between follicular cells in the arrested developed non-mated ovaries. Based on these observations, we postulate that the specific type of ECM, such as type IV collagen between the follicular cells, may influence the development of the follicular cell layers.

Additionally, being a signal molecule, the ECM also regulates cell behaviors such as adhesion, migration, proliferation, and differentiation via binding to integrins.[34] Interestingly, the term "integrin complex" was also significantly enriched in the analysis of DEGs between normally developed mated ovaries and arrested developed non-mated ovaries. Integrins are able to recognize specific ECM proteins, through their extracellular domains, while their intracellular domains bind to cytoskeletal protein such as talin, α-actinin, paxillin, vinculin.[36] This process activates focal adhesion kinase (FAK) signaling pathway,[37] leading to the interaction between ECM and the cytoskeleton, finally resulting in cytoskeleton rearrangement.[36] Notably, cytoskeletal protein such as focal adhesion and actin were also identified in our DEGs dataset. Thus, we reasonably infer the ECM may contribute to regulating cytoskeleton rearrangement between ovarian follicular cells in the normally developed mated ovaries of *S. schlegelii*, which is a key step for follicular cells development.

Furthermore, we observed cell adhesion and migration molecules were significantly enriched in our data. Porcine granulosa cells exhibit a normal round shape when plate on type IV collagen and laminin.[30] This leads us to believe that the ECM could enhance cell adhesion and migration, thereby maintaining the normal morphology of the follicular cells in the normally developed mated ovaries of *S. schlegelii*. In an *in vitro* study using Matrigel, which can mimic the role of ECM, human granulosa cells exhibit a rapid aggregation accompanied by increased gap junctions and cell-cell communication.[38] Gap junctions (Gjs) are intercellular channels used to deliver small metabolites, ions, and second messengers, which are responsible for bidirectional communication between oocytes and follicular cells to promote oocyte development.[39,40] Hence, we suspect the ECM in the normally developed mated ovaries could increase the Gjs between oocytes and follicular cells, establishing a metabolic syncytium that is essential for oocyte development.[41,42]

In addition, we investigated that the cholesterol metabolism pathway was significantly enriched in our data. Sex steroid hormone-related genes were significantly down-regulated and not expressed in the follicular cell layers of the arrested developed non-mated ovaries. Sex steroid hormones, such as estradiol-17β (E2), 11-ketotestosterone (11-KT), and 17α,20β-dihydroxyproterone (DHP), are synthesized from cholesterol by a variety of steroidogenic enzymes in ovarian follicular cells, including the granulosa cells and the theca cells. Genes such as *star*, *hsd17b1*, *cyp17a1*, *cyp19a1a* encode these steroidogenic enzymes and serve as markers for ovarian follicular cells.[43,44] Via ISH of sex steroid hormone-related genes, we confirmed these genes were all expressed in the follicular cells of the normally developed mated ovaries but not in the arrested developed non-mated ovaries due to the dysplasia of follicular cell layers. This finding further confirmed that the follicular cell layers in the arrested developed non-mated ovaries were poorly developed.

In most teleost, E2 plays a primary role in stimulating *vitellogenin* expression in the liver and promoting vitellogenesis in the oocytes.[45] Based on this, we conclude that the underdeveloped follicular cell layers in the arrested developed non-mated ovaries impede synthesis of sex steroid hormones, finally hindering oocyte development. Furthermore, the synthesis of follicular estradiol depends on the coordinated actions of the follicle-stimulating hormone (FSH) and luteinizing hormone (LH), which are pituitary gonadotropin hormones. FSH induces estrogen biosynthesis by regulating the transcription of the aromatase gene (*CYP19A1*) in ovarian granulosa cells.[46] The FSHR expression in the normally developed mated ovaries was also significantly increase than arrested developed non-mated ovaries ($Log_2FC = 1.55$, $p = 4.62E\text{-}06$ in 1224MG vs. 1224NMG; $Log_2FC = 2.49$, $p = 2.90E\text{-}06$ in 0303MG vs. 0303NMG). The LHR expression was also significantly different between normally developed mated ovaries and arrested developed non-mated ovaries ($Log_2FC = 2.13$, $p = 1.53E\text{-}05$ in 0303MG vs. 0303NMG; $Log_2FC = 4.53$, $p = 1.25E\text{-}05$ in 0327MG vs. 0327NMG). Besides, the release of FSH and LH are regulated by gonadotropin-releasing hormone (GnRH) secreted hypothalamus. Compared with brain in the non-mated females carrying arrested developed ovaries, the expression of GnRH was also remarkably higher in the brain of the mated females with normally developed ovaries ($Log_2FC = 4.55$, $p = 0.0002$ in 03MG vs. 03NMG). The sex steroid hormones biosynthesis is generally controlled by the hypothalamus–pituitary–gonadal (HPG) axis.[47,48] However, at the vitellogenic stage, only 3 DEGs were found in the brain between the mated females with normally developed ovaries and the non-mated females with arrested developed ovaries (01MG vs. 01NMG). For the normally developed mated ovaries and arrested developed non-mated ovaries, at the vitellogenic stages, 902 DEGs were found (01MG vs. 01NMG). We suspect that semen could regulate directly ovarian development rather than firstly induce a sequence of neuroendocrine events to promote oocyte development in *S. schlegeli*, furthermore, the ovary response to semen gives a positive feedback regulation on the brain, and stimulates the brain to secret GnRH. In summary, well-developed follicular cells in the ovaries of *S. schlegelii* are vitally important for oocyte development and maturation, ensuring proper operation of the HPG axis.

Semen promotes oocyte development by remodeling communications between follicular cells and oocytes

Based on all observations, we speculate that semen can promote oocyte development in *S. schlegelii* by firstly stimulating the development of follicular cells, which further play vital roles in regulating oocyte development and maturation. This mechanism is quite different from the known mechanisms by which sperm promotes oocyte meiosis in hermaphrodite *C. elegans* or oocyte vitellogenesis in marine invertebrates, semen stimulates ovulation in many vertebrate species. A hypothetical model was proposed for the effects of semen on

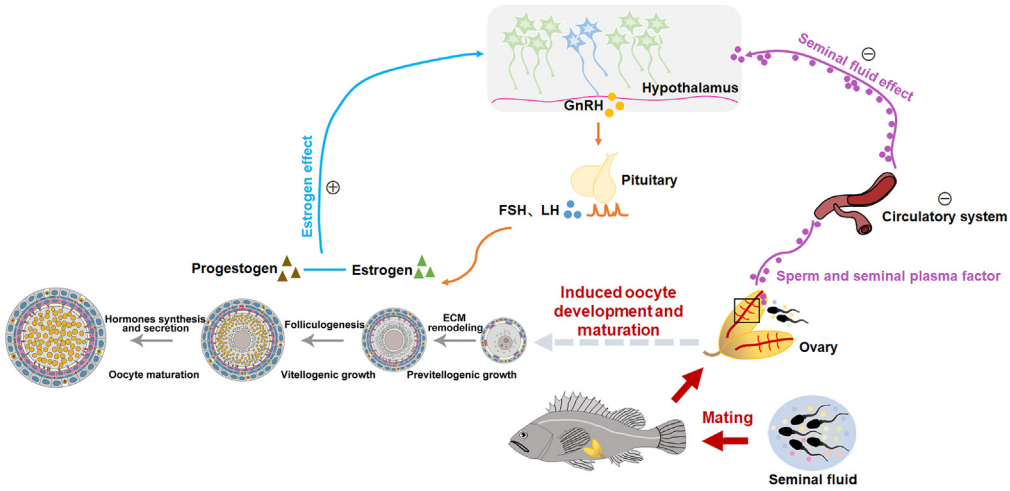

Figure 7. A hypothetical model explaining the effects of semen on oocyte development in the viviparous teleost, *S. schlegelii*

Semen signaling factors facilitate the remodeling of follicular cells by regulating the expression of ECM, a key bridge for establishing connection and facilitating communication between the follicular cells, which further develop and produce steroid to stimulate the development of oocytes. Alternatively, the ovary response to semen may also have a positive feedback effect on the regulation of the hypothalamic-pituitary (H-P) axis, stimulating the release of gonadotropin-releasing hormone (GnRH), follicle-stimulating hormone (FSH) and luteinizing hormone (LH). These hormones, in turn, stimulate the further development of follicular cells, leading to the production of steroids that stimulate of oocyte development.

oocyte development in *S. schlegelii*, as depicted in Figure 7. Semen signaling, delivered to females during mating, firstly, semen promotes the remodeling of ECM between the ovarian follicular cells, establishing connection and enhancing communication between the oocytes and ovarian follicular cells and stimulating the development of oocytes. In contrast, sometimes, when the females don't mate with the males, inadequate ECM remodeling potentially results in failure to establish the connection between the oocyte and ovarian follicular cells. Consequently, the synthesis of sex steroid hormones is detained and estrogen production is insufficient in the follicular cells, which leads to the arrested development of the oocytes. Furthermore, the signaling that the ovary response to semen is transferred to the ovary artery, and through an endocrine action, accesses the H-P axis in the brain, to induce GnRH, FSH, and LH release. FSH and LH stimulate the release of estrogen in the follicular cells, promoting oocyte vitellogenesis and development. Estrogen may also have a positive feedback effect on the regulation of the H-P axis. The mechanism, which could potentially delay maternal investment in offspring until male genetic input has occurred to avoid energy wasting, has not been described in teleost fish. Future study should explore how sperm or semen promotes the growth of oocyte development.

Limitations of the study

We found that semen could promote oocyte development in the viviparous fish *Sebastes schlegelii*. However, in the non-mated group, 39% of individuals still developed normally, suggesting that other factors may contribute to oocyte development. Yet, our data did not reveal these significant factors.

STAR★METHODS

Detailed methods are provided in the online version of this paper and include the following:

- KEY RESOURCES TABLE
- RESOURCE AVAILABILITY
  - Lead contact
  - Materials availability
  - Data and code availability
- EXPERIMENTAL MODEL AND STUDY PARTICPANT DETAILS
- METHOD DETAILS
  - Morphological and histological analysis
  - Ultrastructural analysis
  - TUNEL *in situ* reaction
  - RNA extraction and high-throughput RNA sequencing
  - Transcriptome data processing and qRT-PCR validation
  - Wheat germ agglutinin staining

- *In situ* hybridization
- QUANTIFICATION AND STATISTICAL ANALYSIS

SUPPLEMENTAL INFORMATION

Supplemental information can be found online at https://doi.org/10.1016/j.isci.2024.109193.

ACKNOWLEDGMENTS

This study was financially supported by grants from the Key Research and Development Project of Shandong Province of China (2022ZLGX01), National Natural Science Foundation of China (32070515, 32370564), and Technological Small and Medium-sized Enterprises Innovation Enhancement Project of Shandong Province of China (2023TSGC0638). This work was also supported by High-performance Computing Platform of YZBSTCACC. The funders were not involved in the design of the study and collection, analysis, and interpretation of data and in writing the article.

AUTHOR CONTRIBUTIONS

Y.H.: Funding acquisition, conceptualization, resources, project administration, supervision, and writing-review and editing; Q.Z.: conceptualization and resources; J.Q.: conceptualization; F.Z.: data curation, methodology, project administration, validation, investigation, formal analysis, visualization, and writing-original draft; W.S.: software, formal analysis, and investigation; R.Y.: investigation; C.J.: software and investigation; Y.X.: investigation; Y.S.: methodology; X.G.: investigation; H.S.: investigation; T.N.: software and investigation; X.Y.: resources; and C.S.: resources. All authors gave final approval for publication and agreed to be held accountable for the work performed therein.

DECLARATION OF INTERESTS

The authors declare no competing interests.

Received: July 11, 2023
Revised: November 17, 2023
Accepted: February 7, 2024
Published: February 10, 2024

REFERENCES

1. Yoshida, M., Inaba, K., and Morisawa, M. (1993). Sperm chemotaxis during the process of fertilization in the ascidians *Ciona savignyi* and *Ciona intestinalis*. Dev. Biol. *157*, 497–506. https://doi.org/10.1006/dbio.1993.1152.
2. Miller, R.L. (1975). Chemotaxis of the spermatozoa of *Ciona intestinalis*. Nature *254*, 244–245. https://doi.org/10.1038/254244a0.
3. Shankar, G., Gagan, T.A., Kumari, T.R.S., and Marathe, G.K. (2023). Sperm storage by females across the animal phyla: A survey on the occurrence and biomolecules involved in sperm storage. J. Exp. Zool. B Mol. Dev. Evol. *340*, 283–297. https://doi.org/10.1002/jez.b.23189.
4. Wolfner, M.F. (2002). The gifts that keep on giving: physiological functions and evolutionary dynamics of male seminal proteins in Drosophila. Heredity *88*, 85–93. https://doi.org/10.1038/sj.hdy.6800017.
5. Heifetz, Y., Lung, O., Frongillo, E.A., Jr., and Wolfner, M.F. (2000). The Drosophila seminal fluid protein Acp26Aa stimulates release of oocytes by the ovary. Curr. Biol. *10*, 99–102. https://doi.org/10.1016/s0960-9822(00)00288-8.
6. Heifetz, Y., Tram, U., and Wolfner, M.F. (2001). Male contributions to egg production: the role of accessory gland products and sperm in *Drosophila melanogaster*. Proc. Biol. Sci. *268*, 175–180. https://doi.org/10.1098/rspb.2000.1347.
7. Pondeville, E., Maria, A., Jacques, J.C., Bourgouin, C., and Dauphin-Villemant, C. (2008). *Anopheles gambiae* males produce and transfer the vitellogenic steroid hormone 20-hydroxyecdysone to females during mating. Proc. Natl. Acad. Sci. USA *105*, 19631–19636. https://doi.org/10.1073/pnas.0809264105.
8. Hoshino, R., and Niwa, R. (2021). Regulation of Mating-Induced Increase in Female Germline Stem Cells in the Fruit Fly *Drosophila melanogaster*. Front. Physiol. *12*, 785435. https://doi.org/10.3389/fphys.2021.785435.
9. Bishop, J.D., Manríquez, P.H., and Hughes, R.N. (2000). Water-borne sperm trigger vitellogenic egg growth in two sessile marine invertebrates. Proc. Biol. Sci. *267*, 1165–1169. https://doi.org/10.1098/rspb.2000.1124.
10. Ratto, M.H., Leduc, Y.A., Valderrama, X.P., van Straaten, K.E., Delbaere, L.T.J., Pierson, R.A., and Adams, G.P. (2012). The nerve of ovulation-inducing factor in semen. Proc. Natl. Acad. Sci. USA *109*, 15042–15047. https://doi.org/10.1073/pnas.1206273109.
11. El Allali, K., El Bousmaki, N., Ainani, H., and Simonneaux, V. (2017). Effect of the Camelid's Seminal Plasma Ovulation-Inducing Factor/β-NGF: A Kisspeptin Target Hypothesis. Front. Vet. Sci. *4*, 99. https://doi.org/10.3389/fvets.2017.00099.
12. He, Y., Chang, Y., Bao, L., Yu, M., Li, R., Niu, J., Fan, G., Song, W., Seim, I., Qin, Y., et al. (2019). A chromosome-level genome of black rockfish, *Sebastes schlegelii*, provides insights into the evolution of live birth. Mol. Ecol. Resour. *19*, 1309–1321. https://doi.org/10.1111/1755-0998.13034.
13. Zhao, H., Wang, X., Du, T., Gao, G., Wu, L., Xu, S., Xiao, Y., Wang, Y., Liu, Q., and Li, J. (2021). Sperm maturation, migration, and localization before and after copulation in black rockfish (*Sebastes schlegelii*). Theriogenology *166*, 83–89. https://doi.org/10.1016/j.theriogenology.2021.01.001.
14. Song, W., Xie, Y., Sun, M., Li, X., Fitzpatrick, C.K., Vaux, F., O'Malley, K.G., Zhang, Q., Qi, J., and He, Y. (2021). A duplicated amh is the master sex-determining gene for *Sebastes* rockfish in the Northwest Pacific. Open Biol. *11*, 210063. https://doi.org/10.1098/rsob.210063.
15. MORI, H., NAKAGAWA, M., SOYANO, K., and KOYA, Y. (2003). Annual reproductive cycle of black rockfish *Sebastes schlegeli* in captivity. Fish. Sci. *69*, 910–923. https://doi.org/10.1046/j.1444-2906.2003.00707.x.
16. Xu, X., Liu, Q., Wang, X., Qi, X., Zhou, L., Liu, H., and Li, J. (2021). New insights on folliculogenesis and follicular placentation in marine viviparous fish black rockfish (*Sebastes schlegelii*). Gene *827*, 146444. https://doi.org/10.1101/2021.01.20.427513.
17. Nakagawa, M., and Okouchi, H. (2003). Abnormal spawning of female black rockfish, *Sebastes schlegli*, in the absence of copulation. Saibai Gyogyo Gijutsu Kaihatsu Kenkyu (Japan) *30*, 75–77. https://agris.fao.org/search/en/records/647242e92c1d629bc979305b.
18. Grier, H.J., Uribe, M.C., and Patino, R. (2009). The Ovary, Folliculogenesis, and Oogenesis in Teleosts, 1st Edition (CRC Press). https://doi.org/10.1201/9781482280609-8.

19. Morais, R.D.V.S., Thomé, R.G., Lemos, F.S., Bazzoli, N., and Rizzo, E. (2012). Autophagy and apoptosis interplay during follicular atresia in fish ovary: a morphological and immunocytochemical study. Cell Tissue Res. *347*, 467–478. https://doi.org/10.1007/s00441-012-1327-6.
20. Wei, J., Wang, G., Li, X., Ren, P., Yu, H., and Dong, B. (2017). Architectural delineation and molecular identification of extracellular matrix in ascidian embryos and larvae. Biol. Open *6*, 1383–1390. https://doi.org/10.1242/bio.026336.
21. Schwab, M.E., Javoy-Agid, F., and Agid, Y. (1978). Labeled wheat germ agglutinin (WGA) as a new, highly sensitive retrograde tracer in the rat brain hippocampal system. Brain Res. *152*, 145–150. https://doi.org/10.1016/0006-8993(78)90140-3.
22. Kostrominova, T.Y. (2011). Application of WGA lectin staining for visualization of the connective tissue in skeletal muscle, bone, and ligament/tendon studies. Microsc. Res. Tech. *74*, 18–22. https://doi.org/10.1002/jemt.20865.
23. Mendonça, M.T., and Crews, D. (1990). Mating-induced ovarian recrudescence in the red-sided garter snake. J. Comp. Physiol. *166*, 629–632. https://doi.org/10.1007/bf00240012.
24. Whittier, J.M., and Crews, D. (1986). Ovarian development in red-sided garter snakes, *Thamnophis sirtalis parietalis*: relationship to mating. Gen. Comp. Endocrinol. *61*, 5–12. https://doi.org/10.1016/0016-6480(86)90243-1.
25. Kawasaki, T., Shimizu, Y., Mori, T., Hiramatsu, N., and Todo, T. (2017). Development of artificial insemination techniques for viviparous black rockfish (*Sebastes schlegelii*). Aquaculture Science *65*, 73–82. https://doi.org/10.11233/aquaculturesci.65.73.
26. Ee-Yung, C., Jin, C., and Keun-Kwang, L. (1995). Activities of Hepatocytes and Changes of Protein and Total RNA Contents in Liver and Muscle of *Sebastes schlegeli* with the Gonadal Maturation. Korean Journal of Fisheries and Aquatic Sciences *28*, 338–346. https://api.semanticscholar.org/CorpusID:82017482.
27. Bo, Y., Zhang, W., Lu, J., Wang, Y., and Xu, Y. (2022). Rhythmic expressions of biological clocks and metabolic genes in marine medaka (*Oryzias melastigma*). Aquacult. Res. *53*, 3541–3552. https://doi.org/10.1111/are.15860.
28. Kulczykowska, E., Popek, W., and Kapoor, B.G. (2010). Biological Clock in Fish. https://doi.org/10.1201/b10170.
29. Khan, Z., Mondal, G., Rajiv, C., Sanjita Devi, H., Yumnamcha, T., Dharmajyoti, S., Labala, R., and Chattoraj, A. (2022). Biological Clock and Melatonin: A Crosstalk in the Era of Artificial Light at Night (ALAN) in Fish. Annals of Multidisciplinary Research, Innovation and Technology *1*, 40–46. https://www.researchgate.net/publication/363517885_Biological_Clock_and_Melatonin_A_Crosstalk_in_the_Era_of_Artificial_Light_at_Night_ALAN_in_Fish.
30. Sites, C.K., Kessel, B., and LaBarbera, A.R. (1996). Adhesion proteins increase cellular attachment, follicle-stimulating hormone receptors, and progesterone production in cultured porcine granulosa cells. In Proceedings of the Society for Experimental Biology and Medicine, *212* (Society for Experimental Biology and Medicine), pp. 78–83. https://doi.org/10.3181/00379727-212-43994.
31. Lajus, D., and Alekseev, V. (2019). Fish: Diapause, Dormancy, Aestivation, and Delay in Gonad Development. https://doi.org/10.1007/978-3-030-21213-1_4.
32. Theocharis, A.D., Skandalis, S.S., Gialeli, C., and Karamanos, N.K. (2016). Extracellular matrix structure. Adv. Drug Deliv. Rev. *97*, 4–27. https://doi.org/10.1016/j.addr.2015.11.001.
33. Bosman, F.T., and Stamenkovic, I. (2003). Functional structure and composition of the extracellular matrix. J. Pathol. *200*, 423–428. https://doi.org/10.1002/path.1437.
34. Frantz, C., Stewart, K.M., and Weaver, V.M. (2010). The extracellular matrix at a glance. J. Cell Sci. *123*, 4195–4200. https://doi.org/10.1242/jcs.023820.
35. Brown, H.M., Dunning, K.R., Robker, R.L., Pritchard, M., and Russell, D.L. (2006). Requirement for ADAMTS-1 in extracellular matrix remodeling during ovarian folliculogenesis and lymphangiogenesis. Dev. Biol. *300*, 699–709. https://doi.org/10.1016/j.ydbio.2006.10.012.
36. Geiger, B., Spatz, J.P., and Bershadsky, A.D. (2009). Environmental sensing through focal adhesions. Nat. Rev. Mol. Cell Biol. *10*, 21–33. https://doi.org/10.1038/nrm2593.
37. Hynes, R.O. (2002). Integrins: bidirectional, allosteric signaling machines. Cell *110*, 673–687. https://doi.org/10.1016/s0092-8674(02)00971-6.
38. Richardson, M.C., Slack, C., and Stewart, I.J. (2000). Rearrangement of extracellular matrix during cluster formation by human luteinising granulosa cells in culture. J. Anat. *196*, 243–248. https://doi.org/10.1046/j.1469-7580.2000.19620243.x.
39. Kidder, G.M., and Mhawi, A.A. (2002). Gap junctions and ovarian folliculogenesis. Reproduction *123*, 613–620. https://doi.org/10.1530/rep.0.1230613.
40. Yamamoto, Y., and Yoshizaki, G. (2008). Heterologous gap junctions between granulosa cells and oocytes in ayu (*Plecoglossus altivelis*): formation and role during luteinizing hormone-dependent acquisition of oocyte maturational competence. J. Reprod. Dev. *54*, 1–5. https://doi.org/10.1262/jrd.19178.
41. Winterhager, E., and Kidder, G.M. (2015). Gap junction connexins in female reproductive organs: implications for women's reproductive health. Hum. Reprod. Update *21*, 340–352. https://doi.org/10.1093/humupd/dmv007.
42. Kidder, G.M., and Vanderhyden, B.C. (2010). Bidirectional communication between oocytes and follicle cells: ensuring oocyte developmental competence. Can. J. Physiol. Pharmacol. *88*, 399–413. https://doi.org/10.1139/y10-009.
43. Rajakumar, A., and Senthilkumaran, B. (2020). Steroidogenesis and its regulation in teleost-a review. Fish Physiol. Biochem. *46*, 803–818. https://doi.org/10.1007/s10695-019-00752-0.
44. Tokarz, J., Möller, G., Hrabě de Angelis, M., and Adamski, J. (2015). Steroids in teleost fishes: A functional point of view. Steroids *103*, 123–144. https://doi.org/10.1016/j.steroids.2015.06.011.
45. Kazeto, Y., Tosaka, R., Matsubara, H., Ijiri, S., and Adachi, S. (2011). Ovarian steroidogenesis and the role of sex steroid hormones on ovarian growth and maturation of the Japanese eel. J. Steroid Biochem. Mol. Biol. *127*, 149–154. https://doi.org/10.1016/j.jsbmb.2011.03.013.
46. Parakh, T.N., Hernandez, J.A., Grammer, J.C., Weck, J., Hunzicker-Dunn, M., Zeleznik, A.J., and Nilson, J.H. (2006). Follicle-stimulating hormone/cAMP regulation of aromatase gene expression requires beta-catenin. Proc. Natl. Acad. Sci. USA *103*, 12435–12440. https://doi.org/10.1073/pnas.0603006103.
47. Kumar, P., Behera, P., Christina, L., and Kailasam, M. (2021). Sex Hormones and Their Role in Gonad Development and Reproductive Cycle of Fishes. In Recent updates in molecular Endocrinology and Reproductive Physiology of Fish: An Imperative step in Aquaculture, J.K. Sundaray, M.A. Rather, S. Kumar, and D. Agarwal, eds. (Springer Singapore), pp. 1–22. https://doi.org/10.1007/978-981-15-8369-8_1.
48. Qin, G., Luo, W., Tan, S., Zhang, B., Ma, S., and Lin, Q. (2019). Dimorphism of sex and gonad-development-related genes in male and female lined seahorse, *Hippocampus erectus*, based on transcriptome analyses. Genomics *111*, 260–266. https://doi.org/10.1016/j.ygeno.2018.11.008.
49. Love, M.I., Huber, W., and Anders, S. (2014). Moderated estimation of fold change and dispersion for RNA-seq data with DESeq2. Genome Biol. *15*, 550. https://doi.org/10.1186/s13059-014-0550-8.
50. Nakagawa, M., and Hirose, K. (2004). Individually specific seasonal cycles of embryonic development in cultured broodstock females of the black rockfish, *Sebastes schlegeli*. Aquaculture *233*, 549–559. https://doi.org/10.1016/j.aquaculture.2003.09.019.
51. Grove, B.D., and Wourms, J.P. (1994). Follicular placenta of the viviparous fish, *Heterandria formosa*: II. Ultrastructure and development of the follicular epithelium. J. Morphol. *220*, 167–184. https://doi.org/10.1002/jmor.1052200206.
52. Wagner, G.P., Kin, K., and Lynch, V.J. (2012). Measurement of mRNA abundance using RNA-seq data: RPKM measure is inconsistent among samples. Theory in biosciences = Theorie in den Biowissenschaften *131*, 281–285. https://doi.org/10.1007/s12064-012-0162-3.
53. Patro, R., Duggal, G., Love, M.I., Irizarry, R.A., and Kingsford, C. (2017). Salmon provides fast and bias-aware quantification of transcript expression. Nat. Methods *14*, 417–419. https://doi.org/10.1038/nmeth.4197.
54. Jin, C., Song, W., Wang, M., Qi, J., and He, Y. (2020). Transcriptome-wide Identification and Validation of Reference Genes of Black Rockfish (*Sebastes Schlegelii*) for Quantitative RT-PCR (Journal of Ocean University of China). https://doi.org/10.21203/rs.3.rs-17096/v1.
55. Bensley, J.G., De Matteo, R., Harding, R., and Black, M.J. (2016). Three-dimensional direct measurement of cardiomyocyte volume, nuclearity, and ploidy in thick histological sections. Sci. Rep. *6*, 23756. https://doi.org/10.1038/srep23756.

STAR★METHODS

KEY RESOURCES TABLE

REAGENT or RESOURCE	SOURCE	IDENTIFIER
Antibodies		
Anti-Digoxigenin-AP Fab fragments	Roche	Ref. 11093274910; RRID: AB_2734716
Bacterial and virus strains		
Trans5α Chemically Competent Cell	TransGen Biotech	Cat# CD201
Biological samples		
Sebastes schlegelii	This paper	N/A
Chemicals, peptides, and recombinant proteins		
MS-222	Sigma-Aldrich	Cat# E10521
Hematoxylin	Solarbio	Cat# G1140
Eosin	Solarbio	Cat# G1100
4% Paraformaldehyde (PFA) Solution	Boster	Cat# AR1069
Bouin's Fixative Solution	Phygene	Cat# PH0976
50% glutaraldehyde solution	Sangon Biotech	Order No. A500484
Wheat germ agglutinin (Alexa Fluor 555 conjugate)	Thermo Fisher Scientific	Cat# W32464
Antifade Mounting Medium with DAPI	Beyotime	Cat# P0131
Xylene	Sinopharm Chemical Reagent	Cat# 10023418
Ethanol absolute	Sinopharm Chemical Reagent	Cat# 10009218
DNase I (RNase Free)	Accurate Biology	Code No. AG12001
0.5M EDTA(PH8.0)	Solarbio	Cat# E1170
Lithium chloride	Sangon Biotech	Order No. A610307
DEPC	Sangon Biotech	Order No. B600154
Maleic acid	Sangon Biotech	Order No. A610333
Triethanolamine	Sangon Biotech	Order No. A600970
Blocking Reagent	Roche	Ref. 11096176001
Formamide	Sangon Biotech	Order No. A600212
20X SSC Buffer, DEPC Treated	Sangon Biotech	Order No. B548110
Tween 20	Solarbio	Cat# IT9010
Yeast RNA	Beyotime	Cat# R0038
TRIS	Solarbio	Cat# T8060
NaCl	Sinopharm Chemical Reagent	Cat# 10019318
MgCl2·6H2O	Sinopharm Chemical Reagent	Cat# 10012818
KH2PO4	Sinopharm Chemical Reagent	Cat# 10017618
Na2HPO4	Sinopharm Chemical Reagent	Cat# 20040618
KCl	Sinopharm Chemical Reagent	Cat# 10016318
Proteinase K	Beyotime	Cat# ST532
NBT/BICP Stock Solution	Roche	Ref. 11681451001
Neutral red staining solution	Sangon Biotech	Order No. E607312
Neutral baslam	Shanghai Yuanye Bio-Technology	Cat# S30509
SparkZol Reagent	SparkJade	Cat# AC0101
Trichloromethane	Sinopharm Chemical Reagent	Cat# 10006818
Isopropanol	Sinopharm Chemical Reagent	Cat# 80109218

(*Continued on next page*)

Continued

REAGENT or RESOURCE	SOURCE	IDENTIFIER
Recombinant RNase Inhibitor (Porcine)	Accurate Biology	Code No. AG11608
Critical commercial assays		
RNAclean RNA Kit	Biomed	Cat# RA109
YF®594 TUNEL Apoptosis Kit	UElandy	Cat# T6014L
2X SYBR Green *Pro Taq* HS Premix	Accurate biology	Code No. AG11701
T7 RNA polymerase	Takara	Code No. 2540A
SP6 RNA polymerase	Takara	Code No. 2520A
DIG RNA Labeling Mix, 10X conc	Roche	Ref. 11277073910
MegaFi Fidelity 2X PCR MasterMix	Applied Biological Materials	Cat. No. G897
All-in-One 5X RT MasterMix	Applied Biological Materials	Cat. No. G592
Deposited data		
Sebastes schlegelii star mRNA	CNSA	CNGB Project: CNP0000222
Sebastes schlegelii hsd17b1 mRNA	CNSA	CNGB Project: CNP0000222
Sebastes schlegelii cyp17a1 mRNA	CNSA	CNGB Project: CNP0000222
Sebastes schlegelii cyp19a1a mRNA	CNSA	CNGB Project: CNP0000222
Sebastes schlegelii col4a1 mRNA	CNSA	CNGB Project: CNP0000222
Sebastes schlegelii col4a2 mRNA	CNSA	CNGB Project: CNP0000222
Raw data (transcriptome)	NCBI	BioProject: PRJNA860321
Experimental models: Organisms/strains		
Sebastes schlegelii	This paper	N/A
Oligonucleotides		
See Table S3 for primer sequences	This paper	N/A
Recombinant DNA		
pMD™ 19-T Vector Cloning Kit	Takara	Code No. 6013
Software and algorithms		
Graphpad Prism	V8.0	https://www.graphpad.com/features
fastp	V0.20.0	https://github.com/OpenGene/fastp
hisat2	V2.1.0	http://daehwankimlab.github.io/hisat2
Salmon	V0.7.2	https://github.com/COMBINE-lab/salmon/releases
DEseq2	Love, M. I. et al.[49]	http://www.bioconductor.org/packages/release/bioc/html/DESeq2.html
Integrated DNA Technologies	N/A	http://sg.idtdna.com/pages/home
flashClust	V1.01-2	https://cran.r-project.org/web/packages/flashClust/index.html
FactoMineR	V2.8	https://cran.r-project.org/web/packages/FactoMineR/index.html

RESOURCE AVAILABILITY

Lead contact

Further information and requests of resources and reagents should be directed to and will be fulfilled by the lead contact, Yan He (yanhe@ouc.edu.cn).

Materials availability

This study did not generate new unique reagents.

Data and code availability

- The RNA-seq data in this project have been submitted to NCBI Sequence Read Archive (SRA) under the project number PRJNA860321 and are publicly available.
- This paper does not report original code.
- Any additional information required to reanalyze the data reported in this paper is available from the lead contact upon request.

EXPERIMENTAL MODEL AND STUDY PARTICPANT DETAILS

Two replicates of artificial insemination experiment were conducted in 2020 and 2022 respectively. 65 female adults (average body length 28.68 ± 1.89 cm, average weight 656.39 ± 135.65 g) of *S. schlegelii* were obtained from offshore cages located in the Huangdao district of Qingdao (Shan Dong, China) in 2020. 88 female adults (average body length 32.47 ± 2.46 cm, average weight 880.81 ± 215.20 g) were obtained from Weihai Shenghang Ocean Science and Technology in 2022. For each batch, fish were from the same of fry cohort and reared in cages or in the company facility under the same condition for more than three years, achieving sexually maturity. Natural mating of *S. schlegelii* occurs in later November.[50] Females were separated from males for culturing in October to avoid natural mating. A total of 60 males were cultured separately for fresh semen collection simultaneously, 30 males for each year. 153 females were randomly divided into three groups: the pre-mated group (12 females, pre-mated group also named control group, CT), the mated group (69 females, MG), and the non-mated group (72 females, NMG). Females in the mated group were injected with fresh semen artificially through the genital pore on November 28th, 2020 and November 24th, 2022, following the artificial insemination protocol of *S. schlegelii*.[25] Females in the mated and non-mated groups were cultured in separate cages. The ovaries were collected at various time points, specifically: pre-mating (2020.11.28, 2022.11.24), post-mating (2020.12.24, 2021.1.24, 2023.1.11, 2023.2.15), pre-fertilization (2021.3.3, 2021.3.27, 2023.3.16), post-fertilization (2021.4.17, 2023.4.14), post-gestation (2021.5.12, 2023.5.23). At least three individuals were collected for each group at each time point. The experimental design for artificial insemination is shown in the Figure 1. A portion of the ovarian tissues was immediately frozen in liquid nitrogen and stored at −80°C for RNA extraction and high-throughput RNA sequencing. Another portion of the ovarian tissues was collected for hematoxylin-eosin (HE) staining, transmission electron microscopy (TEM) analysis, TUNEL in situ reaction, wheat germ agglutinin (WGA) staining and *in situ* hybridization (ISH). Prior to sampling, anesthesia was administrated using 120 μg/mL MS-222.

All experimental procedures were conducted in conformity with institutional guidelines for the care and use of laboratory animals. This study was subject to approval by the College of Marine Life Sciences, Ocean University of China Institutional Animal Care and Use Committee.

METHOD DETAILS

Morphological and histological analysis

Biological indicators including body length, body width, body depth, body weight and ovarian weight were measured. The ovarian maturation index (GSI) was calculated as ovarian weight/(body weight-ovarian weight). During the sampling process, photographs of the fish body and ovarian appearances were taken. Ovarian tissues of the three groups (CT, MG, NMG) were fixed with Bouin's solution for 24 h at room temperature. Subsequently, the tissues underwent ethanol gradient dehydration and transparent xylene treatment before being embedded in paraffin. Tissue blocks were then sectioned at 4–5 μm thickness and stained with hematoxylin and eosin. Images were captured using a camera attached to a light microscope (Leica, DFC7000T). The independent-samples *t*-test was performed using Graphpad Prism 8.0 to analyze the significant difference in GSI. Differences with $p < 0.05$ were considered statistically significant. Females with normally developed or arrested developed ovaries were count in the mated and non-mated groups. The chi-square test was performed through Graphpad Prism 8.0 to analyze the correlation between semen and oocyte development.

Ultrastructural analysis

For transmission electron microscopy (TEM), ovarian tissues from normally developed mated ovaries and arrested developed non-mated ovaries were fixed overnight at 4°C in 2.5% glutaraldehyde diluted in 0.1 M PBS (pH 7.4), and subsequently processed following standard procedures as described in a previous study.[51] Semi-thin sections were initially performed to locate the surface of oocytes and its adjacent connective tissues. Subsequently, ultra-thin sections were obtained, sectioned at 60–80 nm thickness. The ultra-thin sections were then observed using a transmission electron microscope, and images were captured on electron image plates.

TUNEL *in situ* reaction

Ovarian tissues from normally developed mated ovaries and arrested developed non-mated ovaries were used for TUNEL (terminal transferase-mediated dUTP nick-end labeling) assay according to the instruction of TUNEL Apoptosis Kit. For the positive control, ovarian tissues were treated with DNase I. Images were captured with a camera attached to a fluorescence microscope (Leica, DFC7000T).

RNA extraction and high-throughput RNA sequencing

Total RNA from ovarian tissues of the three groups (CT, MG, NMG) were extracted using Trizol Regant according to the standard protocol. The quality of RNAs were assessed by Agilent 2100 bioanalyzer (Agilent Technologies, CA, USA). A total of forty-five ovarian samples which were collected from the experiment of 2020 were successfully prepared for RNA library construction and sequencing, including three pre-mated

ovarian samples, eighteen mated ovarian samples and twenty-four non-mated ovarian samples. NEBNext Ultra RNA Library Prep Kit was used for library construction, and the sequencing was conducted using Novaseq 6000 (Illumina, USA). All mated ovaries were normally developed. Among the twenty-four libraries from the non-mated group, nineteen were derived from arrested developed ovaries, while the remaining five were from normally developed ovaries at the maturation stage (three collected on 2021.3.3 and two collected on 2021.3.27).

Transcriptome data processing and qRT-PCR validation

The raw reads from forty-five ovarian samples were preprocessed by removing adaptors and low-quality reads using fastp v0.20.0. Through Fastqc, the clean reads were quality controlled. The clean reads were directly mapped to the genome of *S. schlegelii* through hisat2 v2.1.0 (Table S2). The abundance of RNA, measured in transcripts per kilobase million (TPM),[52] was calculated by Salmon v0.7.2.[53] TPM was used for comparing the ovarian expression differences between the three groups (CT, MG, NMG) at different developmental stages. DEGs (differentially expressed genes) were determined using DEseq2,[49] selecting those with adjusted $p < 0.05$. GO term and KEGG pathway enrichment analysis were conducted, with the top30 terms and pathways displaying adjusted $p < 0.05$ being enriched. Principal component analysis (PCA) and hierarchical clustering of the overall TPM value were performed using the R package between the mated and non-mated ovaries at maturation stage (2021.3.3 and 2021.3.27). qRT-PCR analysis was used for validating the expression patterns of DEGs. Total RNA (1 μg) was reverse transcribed into cDNA using All-in-One 5X RT MasterMix. Specific primers for qRT-PCR were designed using Integrated DNA Technologies (http://sg.idtdna.com/pages/home) shown in Table S3. All qRT-PCR experiments were performed in triplicate on a LightCycler 480 real-time PCR system (Roche, San Francisco, USA), with SYBRGreen employed as the DNA-binding fluorescent dye and ribosomal protein L17 (*rpl17*) gene used as an internal standard.[54] The relative expression level of each gene was calculated using the comparative $2^{-\Delta\Delta Ct}$ method. The qPCR results were then compared with transcriptome data (TPM values) using Graphpad Prism 8 to assess the expression correlation of each gene.

Wheat germ agglutinin staining

For WGA staining, ovarian tissues from the three groups (CT, MG, NMG) were collected and fixed in 4% paraformaldehyde (PFA) at 4°C for 24 h. The fixed ovarian tissues were dehydrated and embedded in paraffin, the tissue blocks were sectioned at 4–5 μm thickness. The tissue sections were subjected to WGA staining along with DAPI. To prepare a stock solution of 1 mg/mL, WGA was dissolved in millipore water. The working concentration used was 1 μg/mL. The paraffin sections were dewaxed, rehydrated and washed in PBS (PH = 7.4). Then, the sections were stained with WGA (1/300 dilution) following the protocol described in previous studies.[20,55] Images were captured with a camera attached to a fluorescence microscope (Leica, DFC7000T).

In situ hybridization

Ovarian tissues from the three groups (CT, MG, NMG) were used for the ISH experiment. The ISH probes of *star*, *hsd17b1*, *cyp17a1*, *cyp19a1a*, *col4a1* gene were amplified from ovarian cDNA using specific primers list in Table S3. The ISH probes were synthesized using a Digoxigenin (DIG)-labeled RNA labeling kit. ISH of ovaries was conducted as previously described,[14] and images were recorded with a camera attached to a light microscope (Leica, DFC7000T).

QUANTIFICATION AND STATISTICAL ANALYSIS

Ovarian maturation index (GSI) was calculated as ovarian weight/(body weight-ovarian weight). All biological indicators were presented as mean ± SD. The independent-samples *t*-test was performed using Graphpad Prism 8.0 to analyze the significant difference in GSI. Differences with $p < 0.05$ were considered statistically significant. Females with normally developed or arrested developed ovaries were counted in the mated and non-mated groups. The chi-square test was performed through Graphpad Prism 8.0 to analyze the correlation between semen and oocyte development.